Reconstruction of reactions $\overline{\mathrm{p}}\mathrm{p} \rightarrow \phi\phi \rightarrow K^+K^-K^+K^-$ at 2230 MeV

K. Götzen

July 21, 2008

Abstract

It is well known that the QCD allows not only conventional hadronic states like mesons ($q\overline{q}$) and baryons (qqq) but also so called hybrid states with valence gluons ($q\overline{q}g$) or even stable states without any valence quark, so called glueballs (gg). There are several expectations for glueball like states at different energies and theory predicts decays to $\phi\phi$. Since the PANDA experiment aims for the confirmation of the real existence of glueball like states this analysis represents the feasibility study for the reconstruction of the decay chain $\overline{\mathrm{p}}\mathrm{p} \rightarrow \phi\phi \rightarrow K^+K^-K^+K^-$.

1 Motivation

2 Analysis Strategy

The primary goal of this study is to proof the feasibility of the reconstruction of exotic states decaying into the favoured decay channel $\phi\phi$. Since no expicit assumption about the exotic particles properties like mass or angular momentum have been made the simulation considered here only comprises non resonant reactions of the type $\overline{\mathrm{p}}\mathrm{p} \rightarrow \phi\phi$ without an intermediate resoncance. As a matter of fact even with resonant reactions in production one has to perform an energy scan around the resonances pole mass to detect an enhancement of the production cross section verifying the resonances existence. Therefore this approach is not really a limitation for the conclusive power of the method.

The procedure is separated in two major steps:

1. Reconstruction of the signal:
   - determination of efficiency of signal
   - estimate background level (signal to noise ratio S/N)
2. Simulation of energy scan:
   - estimate the expected energy dependent cross section with the efficiency measurement from above
   - estimate the required beam time to detect the signal with a significance of 10σ for different assumptions for the signal cross section

3 Reconstruction of Signal

3.1 Simulation and Datasets

Goal of the reconstruction is to determine the number of reactions of the type

$$\overline{\mathrm{p}}\mathrm{p} \rightarrow \phi\phi \rightarrow K^+K^-K^+K^- \tag{1}$$

together with the reconstruction efficiency.

The results presented in this writeup are based on simulations performed with the BaBar like software framework [**?**] which then have been analyzed with the framework internal analysis toolset `Simple Compositions`.

Under the assumption that the efficiency will change very much for different energies in the region around 2.5 GeV signal as well as background events have been generated at $E_{cms} = 2.23$ GeV corresponding to an initial 4-vector

$$P_{\mathrm{init}} = (p_x, p_y, p_z, E \cdot c) = (0, 0, 1432, 2650)\ \mathrm{MeV}. \tag{2}$$

This is region where is has been found evidence for the tensor ($J^{PC} = 2^{++}$) glueball candidate $\xi(2230)$ by the BES experiment [**?**].

Signal events have been generated which the event generator `EvtGen`[**?**] with initial spin $J = 0$ of the $\overline{\mathrm{p}}\mathrm{p}$ system due to technical reasons. Therefore angular distributions are flat and efficiencies can be determined with angular independent accuracy. The simulated decay chain was

$$\begin{aligned} \overline{\mathrm{p}}\mathrm{p} &\rightarrow \phi\phi & (3)\\ \phi &\rightarrow K^+K^- & (4) \end{aligned}$$

The particular decay chain leads to a branching ratio related reduction factor of

$$f_{BR} = \mathcal{B}(\phi \rightarrow K^+K^-)^2 \cdot \underbrace{\mathcal{B}(\mathrm{Glueball} \rightarrow \phi\phi)}_{\text{unknown!}} = (0.492)^2 \cdot x < 0.242 \tag{5}$$

For the time being we will assume the branching ratio to be $\mathcal{B}(\mathrm{Glueball} \rightarrow \phi\phi) = 0.2$ leading to a hypthetical factor $f_{BR} = 0.05$.

Background studies are quite limited up to now since only generic background events generated with the DPM event generator have been considered.

Table 1 summarizes the datasets used for these studies.

Channel	Number of events
$\overline{\mathrm{p}}\mathrm{p} \rightarrow \phi\phi$	50 000
DPM generic	1 000 000

Table 1: Datasets

3.2 Selection

The procdure for the reconstruction was:

1. Select kaon candidates from charged tracks with `veryLoose` PID criterion[1]

[1] PID selection is based on a global likelihood function LH. Available criteria are: `veryLoose` ($LH > 0.2$), `loose` ($LH > 0.8$), `tight` ($LH > 0.95$), `veryTight` ($LH > 0.99$)

2. Create a list of ϕ candidates by forming all combinations of a negative with a positive charged kaon candidate
3. Kinematic fit of the single ϕ candidates with vertex constraint[2]
4. Create $\overline{\mathrm{p}}\mathrm{p}$ candidates by forming any valid[3] combination of two ϕ-candidates

Every of the so formed candidates had to fullfill the follwing requirements:

1. Probability of ϕ vertex fit: $P_\phi > 0.005$
2. Probability of $\overline{\mathrm{p}}\mathrm{p}$ vertex fit: $P_{\overline{\mathrm{p}}\mathrm{p}} > 0.001$
3. ϕ mass window: $|m(K^+K^-) - m_{\mathrm{PDG}}(\phi)| < 12$ MeV/c^2
4. $\phi\phi$ mass window: $|m(\phi\phi) - 2.23\ \mathrm{GeV}/c^2| < 30$ MeV

The latter criterion defines the signal region which is important to determine the efficiency. Fig. 1 shows the corresponding distributions according to the upper selection criteria for signal Monte Carlo data with kaon selection `veryLoose`. The dashed lines in (a) and (d) as well as the box in (b) correspond to the selected mass windows. In plot (a) and (d) a superpostition is shown of all reconstructed candidates as black histogram and candidates failing the so called Monte Carlo Truth (MCT) match[4] as shaded area. While in the final reconstructed $\phi\phi$ candidates the latter one is practically absent, in figure (a) it exhibits a peaking structure. This probably originates from decay trees in which one of the ϕs has been reconstructed correctly but the second one e.g. is composed of another kaon and secondary background track, so that the complete MCT match fails.

In Fig. 2 the same plots are shown for generic background Monte Carlo data. Obviously no ϕ-signal is seen in the invariant mass $m(K^+K^-)$ in plot (a) and the signal window in (d) has no entry. Therefore the conclusion concerning background level from generic hadronic reactions is limited for the time being. Nevertheless a limit is calculated with the assumption of one candidate in the signal region.

To find an optimum for the PID criterion the selection has been repeated for all available criteria

- very loose (VL): $LH > 0.2$
- loose (L): $LH > 0.8$
- tight (T): $LH > 0.9$
- very tight (VT) : $LH > 0.95$

with LH being the global likelihood function computed from information of all PID relevant detectors. The results are summarized in Table 2. Since for every mode no background events were observed in the signal region the optimum would be the most loose selection. The expected signal-to-noise lower limits extracted from this study are between 1:14 and 1:22. These values could be significantly wrong due to the direct influence of the relativ cross section of background with respect to the signal cross section σ_S, which has chosen to be in the order of 10^6. This could be off by up to a factor 1000 assuming $\sigma_S \approx \mathcal{O}(1\ \mathrm{nb})$.

[2]vertex constraint: fit candidates under assumption, that all daughter trajectories originate from a common point in space time.

[3]None of the final state kaons may appear twice in the decay tree.

[4]The Monte Carlo Truth match is the check whether a decay tree has been exactly reconstructed as it was generated.

It should be noted that only the order of magnitude of the efficiency, i.e. $\epsilon \approx$ 20-30 %, is important, since it for the time being only serves as input for the simulation of the energy scan presented in the next chapter.

Channel	rel. X-sec	ϵ(VL)[%]	ϵ(L)[%]	ϵ(T)[%]	ϵ(VT)[%]
Signal	1	30.1	28.5	23.7	18.8
DPM generic	10^6	$< 4.3 \cdot 10^{-4}$	$< 4.3 \cdot 10^{-4}$	$< 4.3 \cdot 10^{-4}$	$< 4.3 \cdot 10^{-4}$
r_{SN}	–	$> 1:14$	$> 1:14$	$> 1:17$	$> 1:22$

Table 2: PID optimization summary

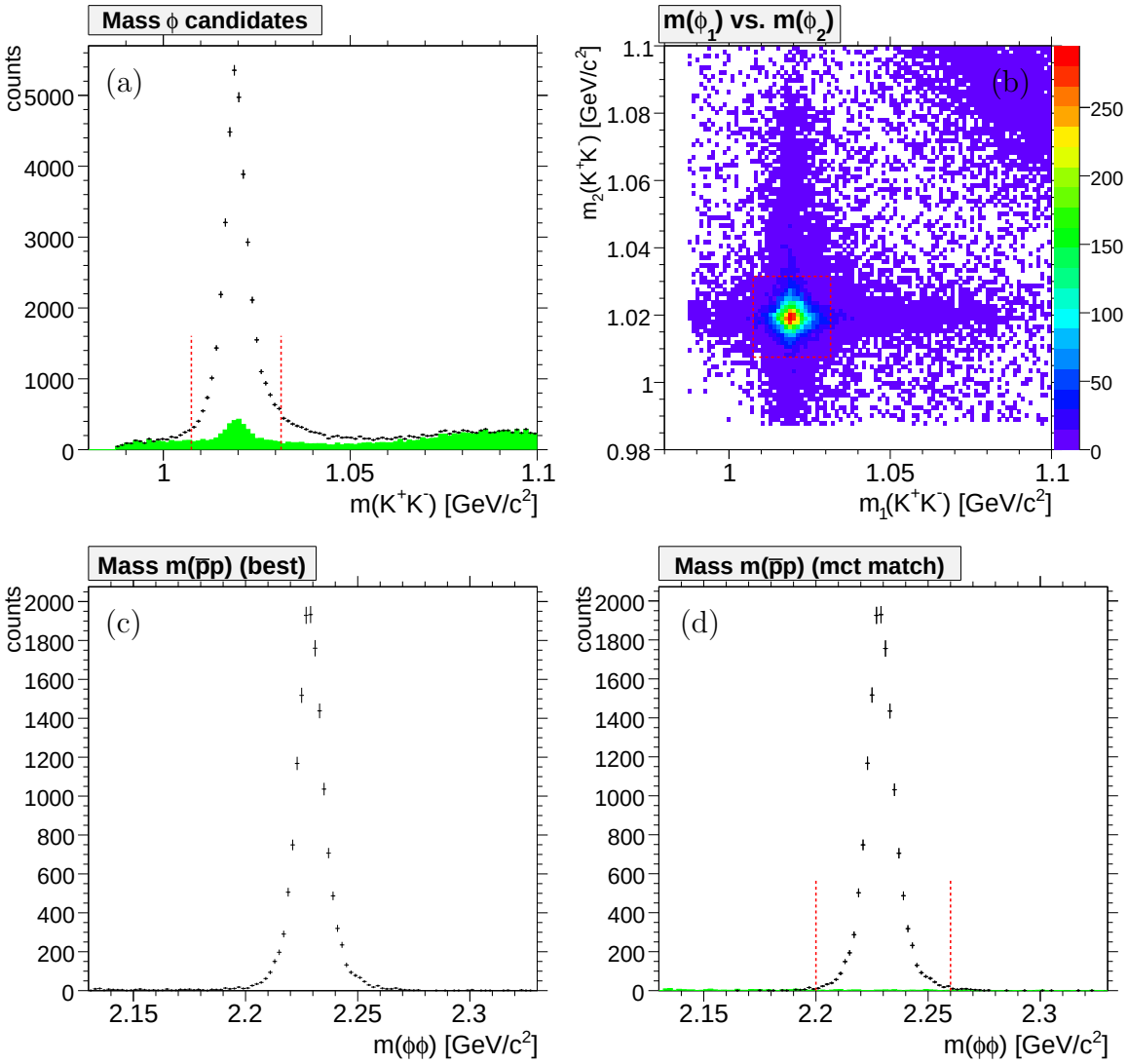

Figure 1: Distributions for reconstructed signal events. (a) Spectrum of the invariant mass $m(K^+K^-)$, (b) 2D plot of invariante masses $m(\phi_1)$ vs. $m(\phi_2)$, (c) invariante mass $m(\phi\phi)$ (best candidate in event) (d) invariant mass $m(\phi\phi)$ with MC truch match. Black histograms correspond to all reconstructed combinations, the shaded area represents combinations failing the MCT match.

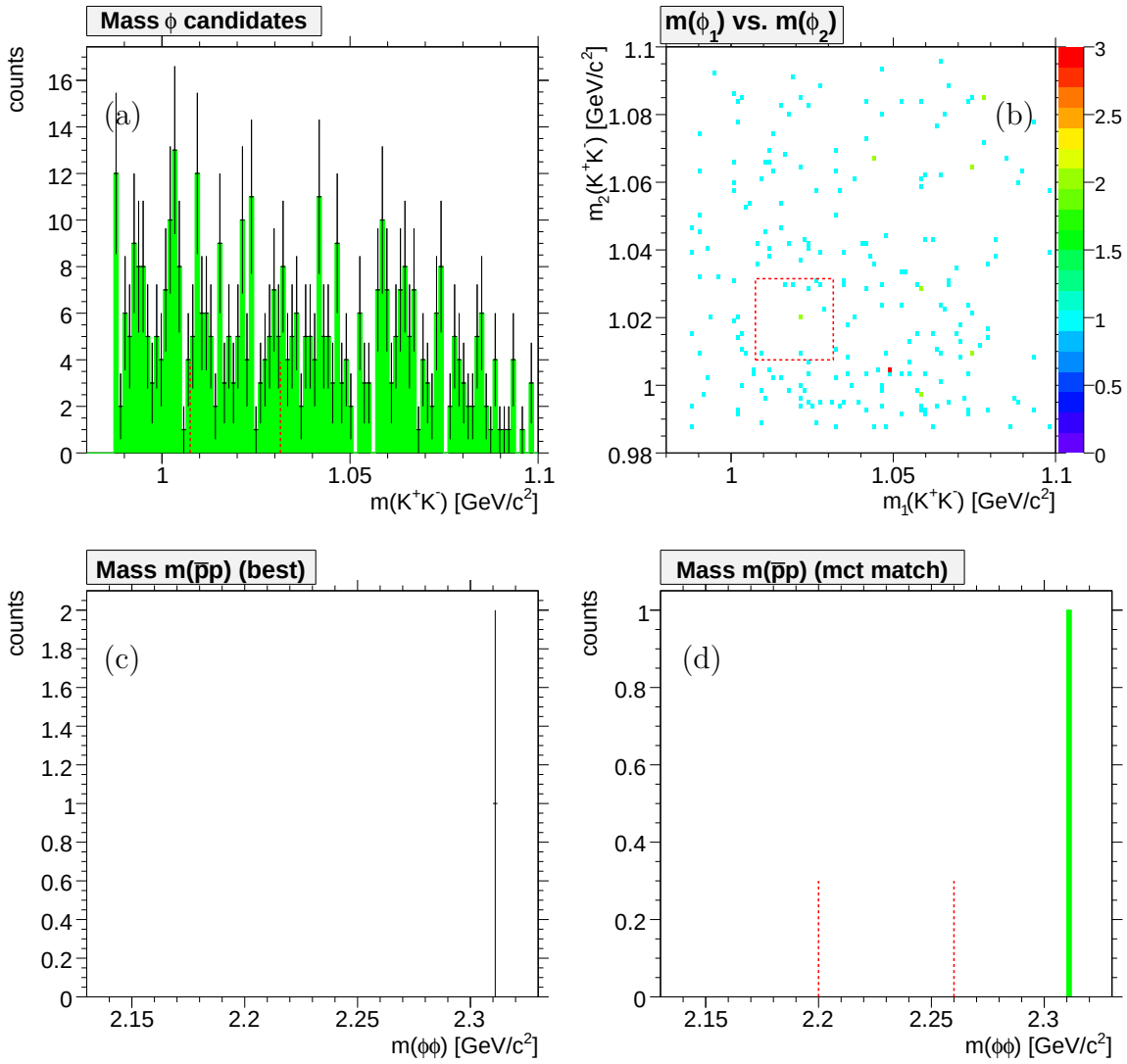

Figure 2: Distributions for reconstructed background events generated with the DPM generator. (a) Spectrum of the invariant mass $m(K^+K^-)$, (b) 2D plot of invariante masses $m(\phi_1)$ vs. $m(\phi_2)$, (c) invariante mass $m(\phi\phi)$ (best candidate in event) (d) invariant mass $m(\phi\phi)$ with MC truch match. Black histograms correspond to all reconstructed combinations, the shaded area represents combinations failing the MCT match.

3.3 Angular Efficiency Dependence

Besides the fact that there will be uncorrelated hadronic background due to misidentification or secondary particles the main obstacle for a high precision detection of a resonant structure in the cross section will probably be the total cross section of non-resonant

$$\overline{\mathrm{p}}\mathrm{p} \to \phi\phi \to K^+K^-K^+K^- \tag{6}$$

reactions which is of the order of $\sigma_{\overline{\mathrm{p}}\mathrm{p}\to\phi\phi} \approx$ 3-4 μb in that energy region. These have exactly the same signature as the signal reactions

$$\overline{\mathrm{p}}\mathrm{p} \to X \to \phi\phi \to K^+K^-K^+K^- \tag{7}$$

and are also kinematically not distinguishable, e.g. by a 4 constraint fit[5]. The only possibilty to disentangle non-resonant from resonant reactions is to perform a spin-parity or partial-wave analysis (PWA). For that purpose it might be crucial to have a 'good' i.e. flat behaviour of the efficiency dependence with respect to the intrinsic appearing angles of the decay. These are

- the decay angle θ_{ϕ_1} of the first ϕ,
- the decay angle θ_{ϕ_2} of the second ϕ and
- the angle ϕ_{plane} between the decay planes of the two ϕ-mesons illustrated in Fig. 3.

The ϕ decay angles have been computed in the following way:

1. boost the ϕ to $\overline{\mathrm{p}}\mathrm{p}$-restframe (3-momentum: $\vec{p}(\phi) \to \vec{p}(\phi)_{\overline{\mathrm{p}}\mathrm{p}}$)
2. boost the K^+ from that ϕ decay to the $\overline{\mathrm{p}}\mathrm{p}$-restframe ($\vec{p}(K) \to \vec{p}(K)_{\overline{\mathrm{p}}\mathrm{p}}$)
3. boost the boosted K^+ to the ϕ-restframe($\vec{p}(K)_{\overline{\mathrm{p}}\mathrm{p}} \to \vec{p}(K)_{\overline{\mathrm{p}}\mathrm{p},\phi}$)
4. $\theta_\phi = \angle\left(\vec{p}(\phi)_{\overline{\mathrm{p}}\mathrm{p}}, \vec{p}(K)_{\overline{\mathrm{p}}\mathrm{p},\phi}\right)$

Since the spin of the initial $\overline{\mathrm{p}}\mathrm{p}$ system $J = 0$ the decay angles of the ϕ's are expected to be flat.

This can be seen in figure Fig. 4 (a) and (c). It is shown the distribution of the cosine of the ϕ mesons decay angle θ_ϕ of the generated Monte Carlo truth particles in black, and the same in red for the reconstructed candidates, here with very loose kaon identification. Dividing the reconstructed by the generated spectrum one gets the angle dependent efficiency distribution. It can be seen clearly that the efficiency is angular independent.

Plot (e) shows the distribution of the angle ϕ_{plane} between the decay planes of two the ϕ mesons and the corresponding efficiency in (f). Also this efficiency behaves 'good' making a potential PWA less difficult later on.

4 Energy Scan and Significance

4.1 Energy Scan

As mentioned briefly in a previous chapter resonances in formation reactions can only be detected via an energy scan around the potential resonances pole mass. Around this position the total

[5]When in general performing exclusive analysis, the signal quality can be enhanced significantly by performing a so called 4 constraint fit to the reconstructed decay tree. This takes into account that the sum of all 4 momenta in the decay tree have to add up to the 4 momentum of the intial system which is basically defined by the precisely know beam energy.

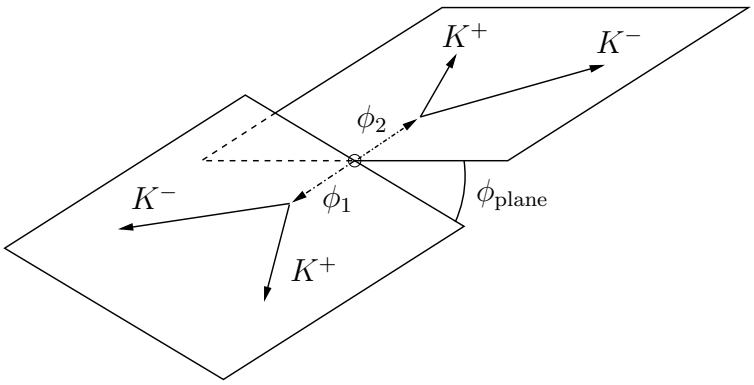

Figure 3: Angle ϕ_{plane} between the decay planes of the two ϕ's.

cross section will be enhanced according to the line shape of the resonance whose intensity could look like a Breit-Wigner distribution

$$BW(m) = A \cdot \frac{1}{\pi} \cdot \frac{\Gamma/2}{(m - m_R)^2 + (\Gamma/2)^2} \tag{8}$$

with Γ and m_R being its total width and pole mass respectively and A being an arbitrary amplitude. This enhancement has to be separated in particular from the non resonant part of the total cross section. The JETSET experiment performed a measurement of exactly this total inclusive cross section of the reaction $\overline{\text{p}}\text{p} \to \phi\phi$ leading to a value $\sigma_{\phi\phi} \approx$ 3-4 μb, as shown in Fig. 5. For the following studies the empirical line fit shown has been considered as the background level upon which the signal shape has to be detected. The curve explicitly was chosen as

$$\sigma_{\text{non-res}}(m) = a + b \cdot m \tag{9}$$

with parameter values $a = 92.8\,\mu$b and $b = -40\,\mu\text{b}/(\text{GeV}/c^2)$.

Figure of merit was to determine the beam time necessary to measure the signal cross section with a significance $S = \sigma/\delta\sigma$ of 10σ, for now neglecting the background considerations for generic events discussed in the last chapter.

The procedure for that purpose was:

1. Assumptions for parameters:
   - Resonance pole mass: $m_{\text{pole}} = 2235$ MeV/c^2
   - Resonance full width: $\Gamma = 15$ MeV/c^2
   - Resonance branching ratio to signal channel: $\mathcal{B}(\xi \to \phi\phi) = 0.2$
   - Integrated luminosity: $\mathcal{L} = 8.8$ pb^{-1}/day
   - Energy window: ± 50 MeV around pole mass
   - Number of equaly distributed scan positions: $n = 25$
   - Reconstruction efficiency of $\phi\phi$ channel: $\epsilon = 0.25$
2. Vary signal cross section σ_S at pole mass between 1 nb and 1 μb
3. Determine the approximate total beam time T_{beam} for the complete measurement to achieve significance of 10σ for the cross section measurement:

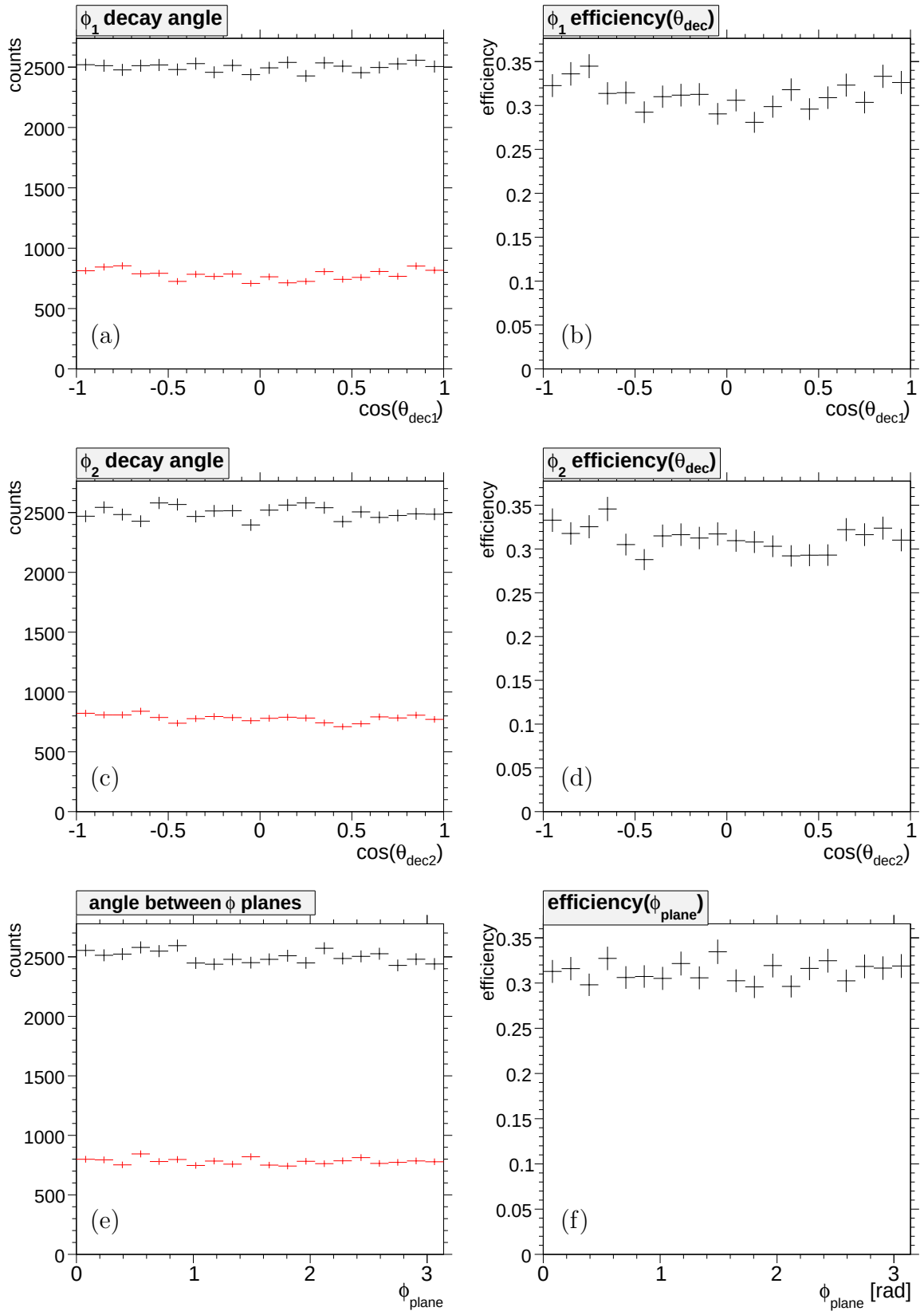

Figure 4: (a) ϕ_1 decay angle $\cos(\theta_{\phi_1})$, (c) ϕ_2 decay angle $\cos(\theta_{\phi_2})$, (e) angle between decay planes. The black histograms show the generated MCT distributions, the red show the same for reconstructed candidates. Dividing the red by the black histogram results in the corresponding angular efficiencies (b), (d) and (f).

- Vary value T_{beam} arbitrarily an apply following steps until significance is 10σ
- Estimate number of expected background entries for each scan energy $E_i = m_i \cdot c^2$ as

$$B_i = \sigma_{\text{non-res}}(m_i) \cdot \epsilon \cdot \frac{T_{\text{beam}}[d] \cdot \mathcal{L}}{n} \tag{10}$$

- Estimate number of expected signal entries for E_i as

$$S_i = \frac{BW(m_i)}{BW(m_{\text{pole}})} \cdot \sigma_S \cdot \epsilon \cdot \mathcal{B}(\xi \to \phi\phi) \cdot \frac{T_{\text{beam}}[d] \cdot \mathcal{L}}{n} \tag{11}$$

- Set contents of bin number i of the scan histogram to $c_i = (S_i + B_i) \pm \sqrt{S_i + B_i}$
- Fit sum of signal function Eq. 8 and background function Eq. 9 to resulting histogram and compute the significance as $A/\delta A$, where A is the fitted amplitude for the resonant part of the fit model.

It turns out that the results reasonably behave according to statistic expectation, i.e. twice the beam time results in a precision improved by a factor $\sqrt{2}$. Fig. 6 and Fig. 7 show the corresponding plots with the fits performed to the total cross section (left column) as well as to the estimated signal cross section determined as the difference of the total cross section and the background expectation computed from Eq. 9 (right column). Both fits agree quite reasonable as expected. It seems surprising that in particular in Fig. 6 (a), (c) and (e) no signal is visible at all whereas the fit result has that high significance. This is due to the extreme high precision of the data points reflected in the corresponding difference plots on the right hand side. Of course this evidently depends on the certainty of signal and background line shapes.

Table 3 summarizes the results for the studies above. The necessary beam times to achieve an accuracy of 10σ significance vary from unfeasible hundreds to thousands of days with assumed signal cross section of $\sigma_S < 10$ nb down to comfortable 'far less than a day' time windows for signal cross sections $\sigma_S > 100$ nb.

It shall be stressed again that the results are too optimistic since strongly idealized by the assumption of the correctness of the knowledge about the total inclusive cross section measurement. Therefore the given beam time estimates might be considerably sensitive to the uncertainties which clearly can be observed in Fig. 5.

This is demonstrated in Fig. 8. In plot (a) the function given by Eq. 9 is displayed as blue curve, in (b) a third order polynomial

$$\sigma_{\text{non-res, 2}}(m) = a + b \cdot m + c \cdot m^2 + d \cdot m^3 \tag{12}$$

with parameter values

$$a = 6994.1445218522731 \tag{13}$$
$$b = -9275.8154735643038 \tag{14}$$
$$c = 4119.5568771324297 \tag{15}$$
$$d = -612.43386225880545 \tag{16}$$

is shown which was used to model a curve very close to the original one. In fact one can hardly see any difference of the shape directly.

With this modified total inclusive cross section model the procedure from above has been repeated, but the resulting distributions still have been fitted with the linear model. The results are presented in plots (c) - (f). Where for the high cross section $\sigma_S = 1000$ nb the significance of the measurement is almost conserved (c, d), the fits for the low cross section scenario (e, f) with $\sigma_S = 10$ nb are completely spoiled by assuming the inappropriate model.

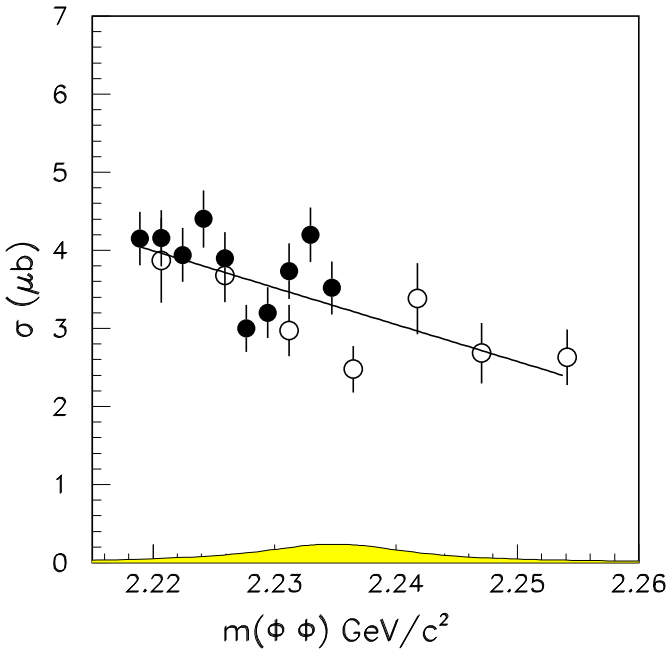

Figure 5: Cross section for the reaction $\overline{\mathrm{p}}\mathrm{p} \to \phi\phi$ measured by the JETSET experiment. The yellow curve represents a Breit-Wigner resonance, whose amplitude is at 95% c.l. upper limit for the production of $f_J(2230)$ at a mass of 2235 MeV/c^2 and a width of 15 MeV/c^2 [**?**].

Signal cross section σ_S [nb]	Total beam time T_{beam} ($\approx$)
1	5000 d
5	200 d
10	50 d
100	12 h
500	0.5 h
1000	7.2 min

Table 3: Beam times needed to achieve a significance of 10σ.

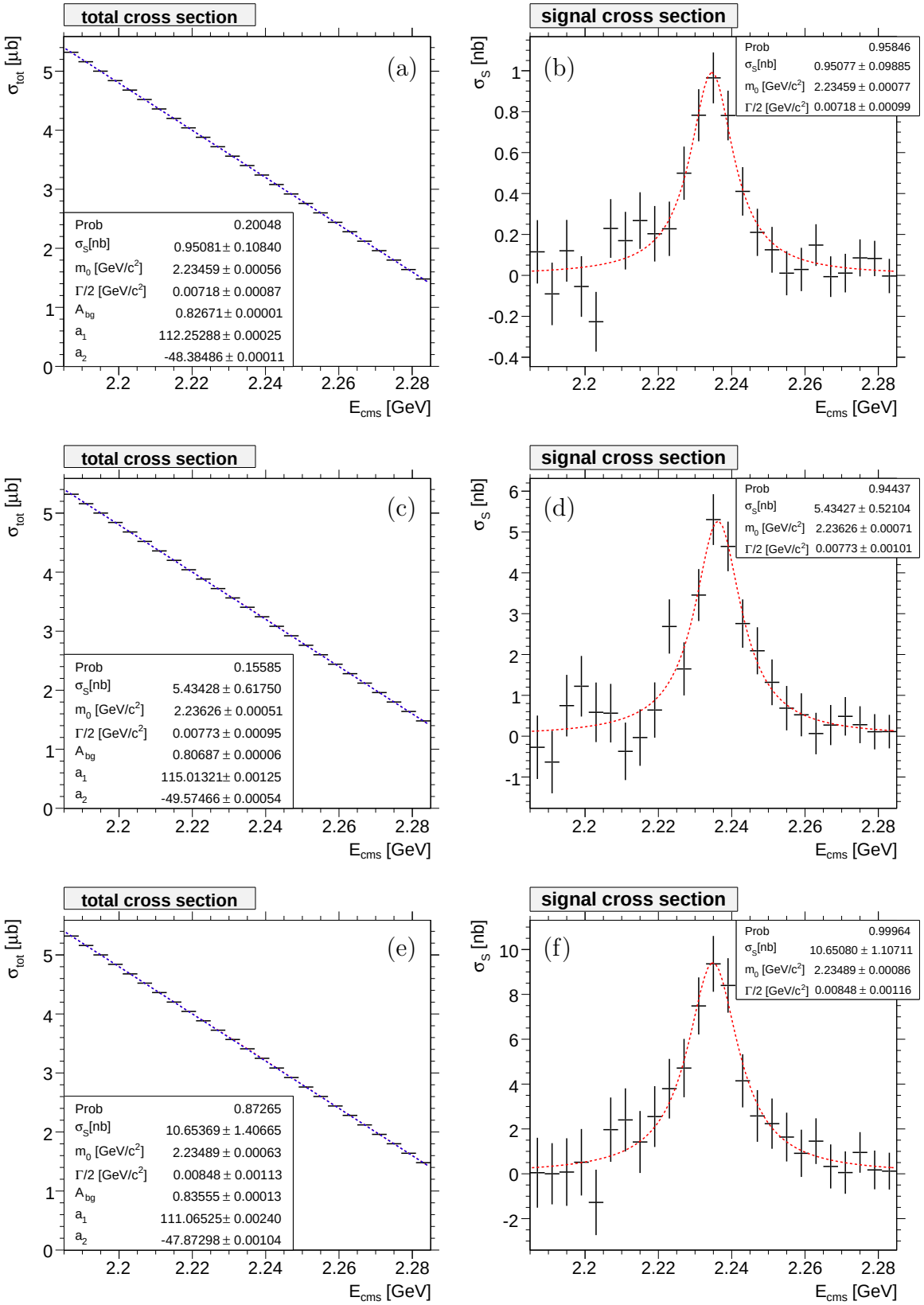

Figure 6: Fits to the total cross section (left column) and the derived signal cross section (right column) for (a, b) $\sigma_S = 1$ nb, (c, d) $\sigma_S = 5$ nb and (e, f) $\sigma_S = 10$ nb for scans with beam times according to Table 3.

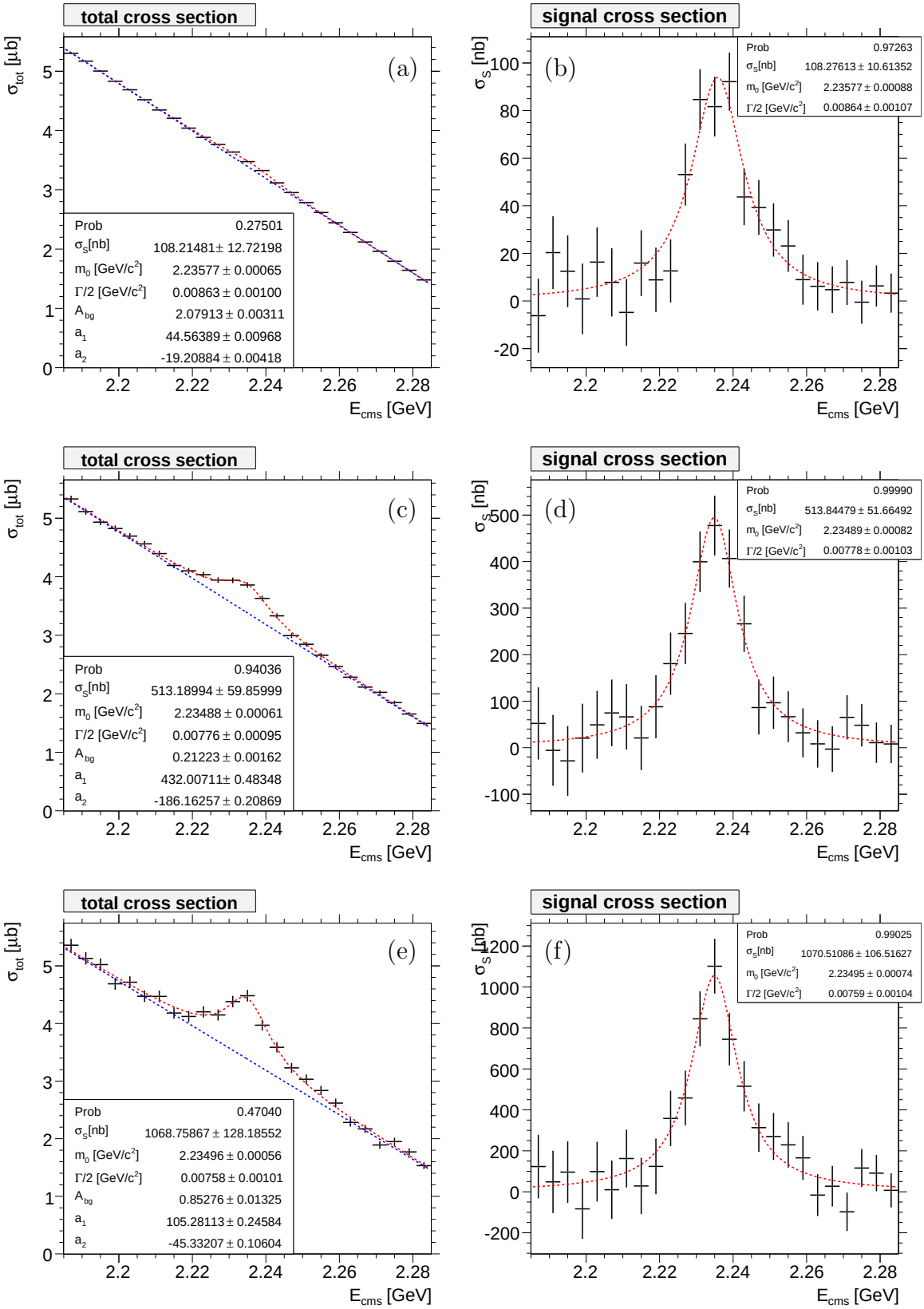

Figure 7: Fits to the total cross section (left column) and the derived signal cross section (right column) for (a, b) $\sigma_S = 100$ nb, (c, d) $\sigma_S = 500$ nb and (e, f) $\sigma_S = 1000$ nb for scans with beam times according to Table 3.

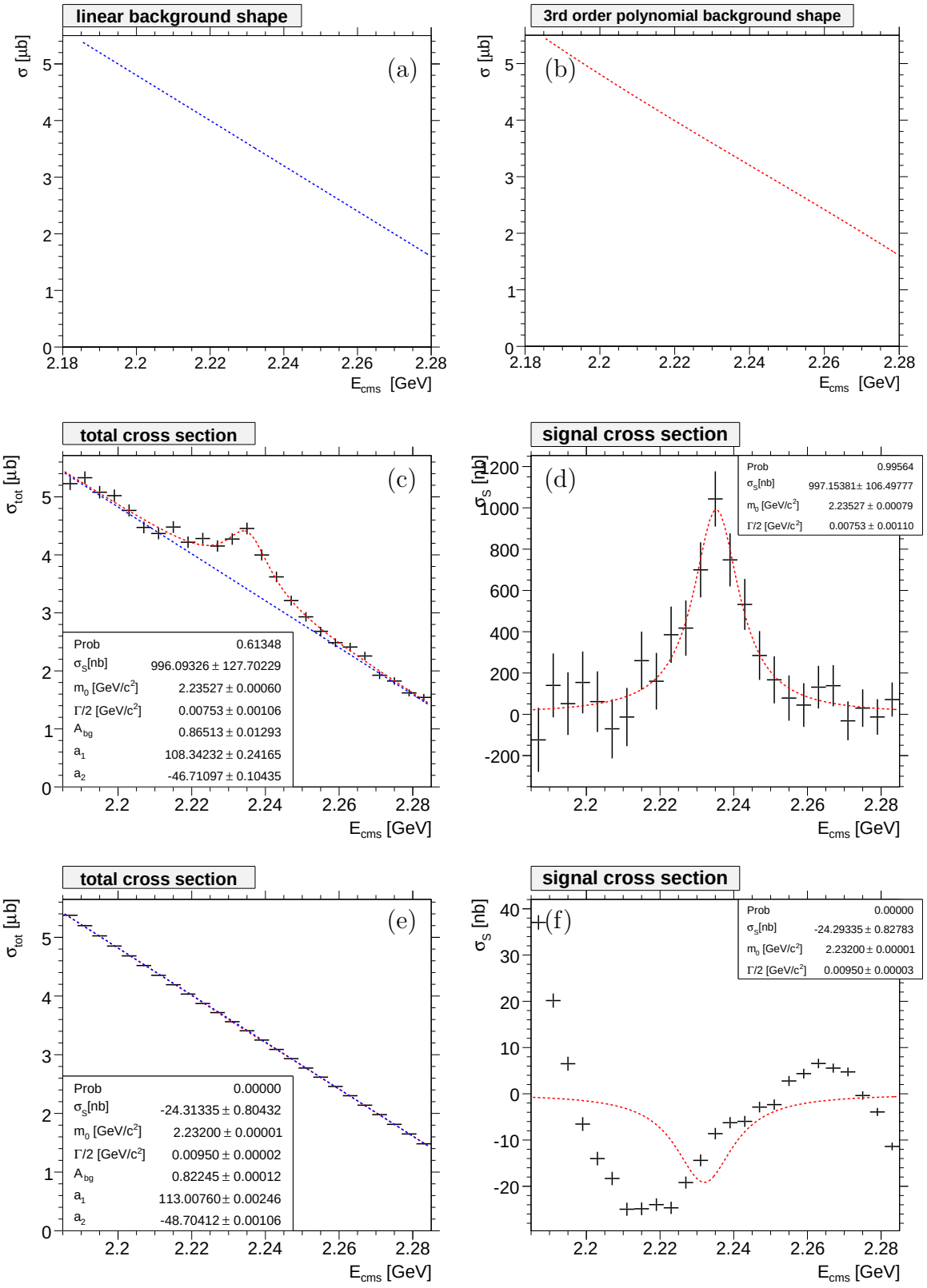

Figure 8: Impact of using wrong background for the significance. (a) linear shape Eq. 9, (b) 3rd oder polynomial shape Eq. 12, fit to total cross section for $\sigma_S = 1000$ nb (c) and $\sigma_S = 10$ nb (e), fit to signal cross section for $\sigma_S = 1000$ nb (d) and $\sigma_S = 10$ nb (f). The wrong shape lets the fit fail completely in the latter two cases. Compare with Fig. 6 (e) and (f).